

Effect of surface treatment on fatigue behavior of metal/carbon fiber laminates

R. S. Almeida · C. A. Damato · E. C. Botelho ·
L. C. Pardini · M. C. Rezende

Received: 18 June 2007 / Accepted: 6 February 2008 / Published online: 11 March 2008
© Springer Science+Business Media, LLC 2008

Abstract The tension–tension fatigue behavior of metal/fiber laminates (MFLs) has been investigated. These MFLs were produced with carbon fiber and by treating the aluminum foil to promote adhesion bonding by two methods: sulfuric–boric–oxalic acid anodization (SBOA) and chromic acid anodization (CAA). The surface treatments were evaluated by scanning electron microscopy (SEM) techniques and roughness measurements. It was observed that MFL specimens produced with SBOA treatments presents comparable mechanical results when compared with MFLs produced with CAA treatment. Microstructural observations of the fracture surfaces by SEM show hackle formation is the predominant damage mechanism.

Introduction

In the last few years, metal/fiber laminates (MFLs) have imposed themselves as versatile, high-performance, and economical materials in aeronautical industry. MFLs were originally developed by the Delft University of Technology at the beginning of 1980 [1]. These hybrid composites are obtained from a sheet of a high-strength aluminum alloy

and a fiber/epoxy layer. These materials can be divided into the three groups: ARALL, GLARE, and CARALL, due to the different fiber-adhesive layers used, i.e., aramid, glass, and carbon fibers, respectively [1].

CARALL laminates consists of thin layers of carbon fiber/epoxy (CF/E) prepreg sandwiched between aluminum sheets. This class of materials offers higher modulus, higher tensile strength, and lower density than 2024-T3 alloy. Figure 1 depicts a CARALL composite used in this study as an example of a metal–fiber laminate. These materials have outstanding fatigue resistance and they are promising candidate for the structural materials of advanced aircraft [2–5].

In addition to the importance of reinforcement and matrix in polymer composites, the adhesion between the composite laminae and the aluminum foil is a key issue for the overall metal–fiber laminate performance. An adequate surface treatment of the aluminum alloy is required to assure a good mechanical bond between the epoxy and aluminum surface. Considerable research has been carried out in this area. To improve the surface activity of aluminum alloys, the most common method in use is the chromic acid anodization (CAA) as surface treatment. This treatment provides a good interface between fiber and metal, but presents serious environmental problems due to the chrome toxicity. To solve this problem, a new anodization process called sulfuric–boric–oxalic acid anodization (SBOA) has been developed [6–9]. To evaluate the effectiveness of the surface treatment used for a metal surface modification, the most common techniques are contact angle and roughness measurements [10–12].

In service, composite structures are often subjected not only to static and impact loads, but also to fatigue loads. Fatigue loading creates fatigue damage, which in turn decreases the in-plane mechanical properties of the

R. S. Almeida
Depto de Engenharia Mecânica e Aeronáutica, Instituto
Tecnológico de Aeronáutica—CTA, Sao Jose dos Campos,
Sao Paulo, Brazil

C. A. Damato · E. C. Botelho (✉)
Department of Materials and Technology, São Paulo State
University, Guaratingueta, Sao Paulo, Brazil
e-mail: ebotelho@feg.unesp.br

L. C. Pardini · M. C. Rezende
Divisão de Materiais, Instituto de Aeronáutica e Espaço, CTA,
Sao Jose dos Campos, Sao Paulo, Brazil

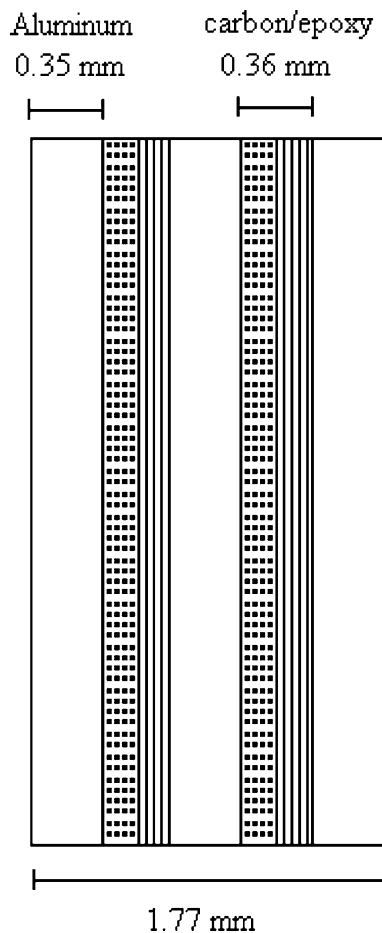


Fig. 1 Schematic view in the thickness direction of a CARALL

composite (strength and stiffness). Under fatigue loads, metals exhibit a nucleation and then propagation of one dominant crack, until failure occurs. On the other hand, fatigue failure mode of composites consists of many modes including matrix cracking, fiber breakage, fiber-matrix debonds, void growth, and delamination. Isolated or a combination of these failure mechanisms may lead to a reduction of the overall modulus and strength. Therefore, fatigue failure is a progressive process during which the overall modulus and strength decrease progressively until their values can no longer resist the applied load and hence total failure occurs [13–20]. The use of textile fabrics has offered a lower cost to composite manufacturing and a higher damage tolerance in impact loading. Failure in woven fabric composites is initiated by fiber–matrix debonds in fiber bundles oriented transversely to the loading direction. In the main directions (weft or warp direction), the final failure is strongly determined by the fiber bundles oriented parallel to the loading direction. The fatigue properties of woven fabric composites are also influenced by the loading direction, stress concentrations around notches and holes, and by the ductility of the matrix [20–24].

The fatigue crack growth of CARALL can be characterized by the growth of two damage mechanisms, i.e. crack growth in the aluminum and delamination growth between the aluminum and composite layer core. Both rates are interrelated under fatigue loading. If fatigue cracks occur in the aluminum layers of a laminate, the fibers remain intact and bridge the crack. The fiber bridging reduces the crack opening displacement and the stress intensity factor at the crack tip. Consequently, the fatigue crack growth rate is reduced [25].

In the present work, the influence of SBOA and CAA treatments used during the metal/carbon fiber laminates processing on the fatigue behavior was investigated. In addition, the treatment morphology was also investigated by using scanning electron microscopy (SEM) and roughness measurements.

Experimental

Materials

Carbon fiber/epoxy prepreg was used for composite preparation. It was supplied by Hexcel Co. The fiber reinforcements were plain weave fabrics. Aluminum alloy 2024-T3 sheets were supplied by Empresa Brasileira de Aeronáutica (EMBRAER), São José dos Campos, Brazil.

A proper surface preparation of aluminum is essential for its successful bonding. Both the initial bond strength and the subsequent bond durability are critically dependent on the interaction between the primer, adhesive, and the pretreated adherent surface. Aluminum surfaces were prepared for bonding by chromic acid anodizing (CAA) and SBOA processes. These acid etching and anodizing processes generate microrough morphologies, which have been shown to yield the best overall bond durability.

Composites processing

The hybrid laminate was prepared by stacking alternating laminae of the prepreg (fiber and epoxy) and the aluminum sheet (Al). The composite was coded as 3/2–0.3, which means three layers of aluminum and two layers of fiber/epoxy prepreg, having the aluminum layer 0.3 mm thick.

During the molding process, the fiber/epoxy prepreg laminae are stacked in between the aluminum layers. Cure preparation involves primarily the bagging of the part and the cutting and placement of many ancillary materials. After the lay-up process, the laminate is vacuum bagged. The laminate is then placed in an autoclave to cure the resin system and bonding the aluminum to the prepreg layer. The curing cycle involved heating at 2.5 °C/min to 120 °C and holding at this final temperature for 1 h. The

pressure and the vacuum used were 0.69 and 0.083 MPa, respectively. The top and the bottom face of the composite are aluminum sheets. The fiber/epoxy layers between the metal sheets fills the gaps, providing load transfer.

Tensile tests

The tensile tests were done according to ASTM-D 3039-76. Ten specimens were tested for each type of laminate (metal–fiber laminate and CF/E composite). The dimensions of the specimens were $247.0 \times 25.4 \times 2.00 \text{ mm}^3$ (length \times width \times thickness). The tests were performed in an Instron mechanical testing machine using a test speed of 1.27 mm/min to establish the strength values. Tensile strain was measured by stacking strain gages, placed at the center of the specimen.

Fatigue tests

Fatigue tests were performed on an Instron fatigue machine at constant amplitude, according to ASTM E 466. Fatigue tests were carried out at different maximum stress ratios S_{\max} ($=\sigma_{\max}/\sigma_{\text{ult}}$). The fatigue stress ratio ($R = \sigma_{\min}/\sigma_{\max}$), was 0.1. The σ_{\max} and σ_{\min} are the maximum and minimum applied stresses, respectively, and σ_{ult} is the ultimate strength of the composites.

Morphological evaluation

The aluminum 2024-T3 alloy treated by SBOA and CAA methods, and the metal/fiber specimens, were analysed by optical microscopy after tensile and fatigue tests. The morphological analysis was performed in a SEM Zeiss 950 model microscope and in the optical microscopy (NIKON microscopy), model EPIPHOT 200. To evaluate the morphology of the specimens, it was used an ultrasound equipment from Automation Industries, model Reflectoscope S 80. The roughness analyses were carried out by using a Perthen laser rugosimeter, from Perthen Company (Germany), using a RHT6-50 pointer by analysing five different regions of the sample.

Results and discussion

Aluminum surface treatment

Morphological evaluation of surface treated and untreated specimens of aluminum 2024-T3 were carried out by SEM micrographs, as shown in Fig. 2. Figure 2b and c shows the pinholes produced after the CAA and SBOA treatment processes over the surface of the aluminum 2024-T3 alloys. According to Fig. 2, it appears that the size distribution and

the shape of pinholes are related to the surface treatment performed on the aluminum 2024-T3 alloy.

While SEM provides valuable information on surface structure and morphology, this technique does not give complete information on changes in the magnitude of surface roughness. Profilometry data can provide an

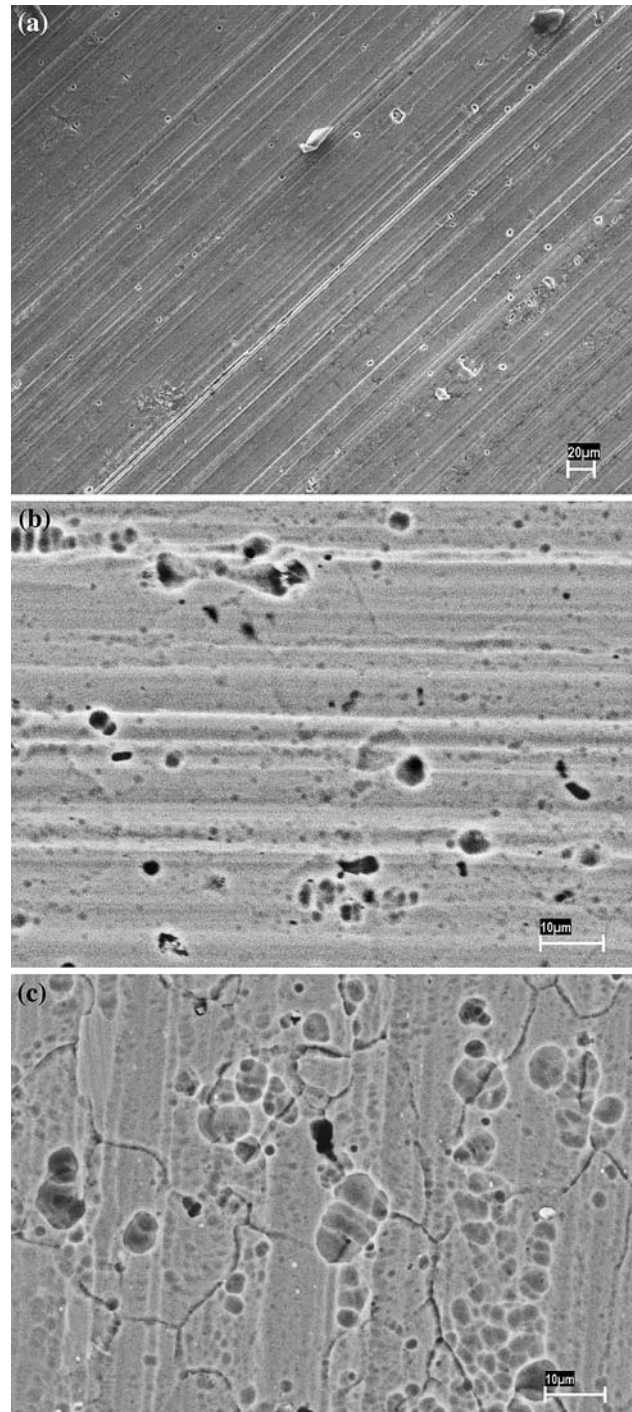


Fig. 2 SEM micrographs of aluminum 2024-T3 alloys: (a) untreated; (b) chromic acid anodization treatment; and (c) sulfuric chromic acid etching treatment

indication of the dominant surface features and whether the features change in size as a result of the surface treatment. Experiments were first performed with untreated aluminum 2024-T3 specimens to compare the roughness associated with different surface treatments (CAA and SBOA). A number of statistical parameters were employed for analysing the roughness data taken with the profilometer. The arithmetic average roughness, R_a , was the key parameter used when comparing roughness trends for the different surface treatment methods [6].

Table 1 shows the roughness values for untreated and treated aluminum 2024-T3 specimens. As can be observed, aluminum specimens presented the same roughness values (~ 0.400 , 0.470 , and $0.440 \mu\text{m}$ for untreated Al, CAA, and SBOA treated specimens, respectively). These values are close to the values found in the literature (between 0.1 and $10 \mu\text{m}$) [6, 26].

Processing evaluation

Figure 3 presents a cross section of the MFL studied in this work. The distinct layers of the polymer composite laminae and the aluminum foil are seen. The thickness of the polymeric composites between the aluminum 2024-T3 layers, is 0.36 mm (carbon fiber). SEM evaluation shows that there is an adequate consolidation between the fiber reinforcement/epoxy resin and the metal layer during processing. Ultrasound C-scans of the laminates studied no detected regions with voids or delamination, showing a homogeneous laminate.

Tensile tests

Table 2 shows the results of the tensile strength and modulus of MFL. According to this table, the rupture strain for CARALL treated by CAA and SBOA and CF/E laminate occurred at strains of about 1.6% , 1.6% and 1.7% , respectively. For these specimens, can be considered that composite components (fiber and matrix) behave elastically until the initial matrix cracking and additionally, transverse stiffness (fibers of 90° toward loading direction) contribution to axial stiffness is negligible.

As can be observed in Table 2, the tensile strength values for CF/E composite and CARALL treated by CAA and SBOA laminate were around 1160 MPa , and 579 and 613 MPa , respectively. In this work, it was observed that

Table 1 Roughness values obtained by the specimens studied

Parameter	Untreated	Chromic acid anodized (CAA)	Sulfuric chromic acid etched (SCAE)
Roughness— R_a	0.400	0.470	0.440

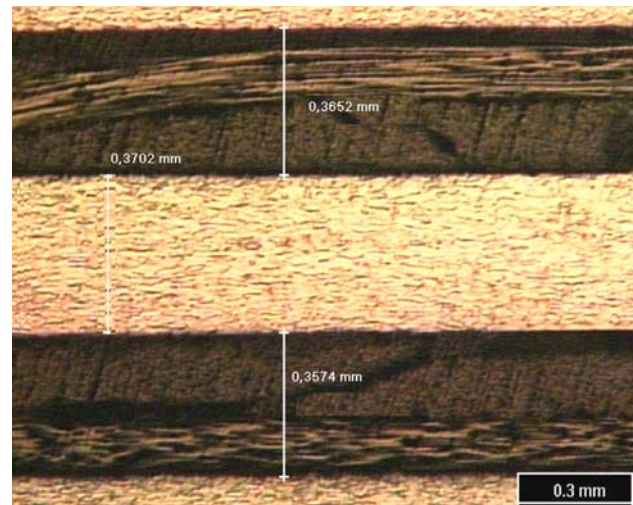


Fig. 3 Optical microscopy of CARALL laminate

Table 2 Tensile results of metal/fiber laminates studied

Laminate	σ (MPa)	ε (%)	E (GPa)
Carbon fiber/epoxy	1160	1.7	67.2
CARALL—CAA	579	1.6	56.1
CARALL—SBOA	613	1.6	56.3

the stress/strain curves for the CARALL composites are predominantly influenced by the aluminum. Therefore, when compared both treatments there is no significant differences on stress values (difference of around 5%).

The elastic modulus, obtained from tensile test of aluminum and CF/E composites are 70 and 67.2 GPa , respectively [26]. Therefore, the elastic modulus of CARALL (around 56 GPa) reflects a contribution from the individual materials resulting in a decrease of mechanical properties (around 20%). When compared both treatments, it was observed no significant differences between the tensile modulus (difference of around 3%).

Fatigue tests

In many fatigue studies, the performance of materials is analyzed by investigating the relationship between the fatigue load (either applied stress or applied strain) and the fatigue life (or number of cycles to failure). The applied fatigue stress can be expressed either as the maximum fatigue stress, or as a normalized value of the maximum fatigue stress σ . This normalized applied stress σ is the ratio of the maximum fatigue stress to the ultimate quasi static or strength of the composite. The normalized applied stress is often used to compare two or more materials against different values of ultimate stress.

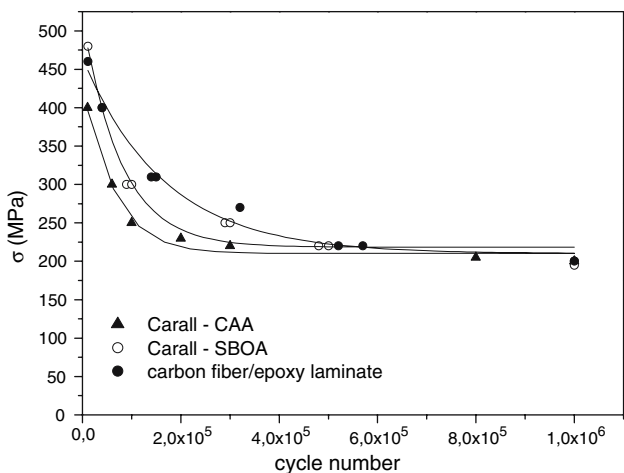


Fig. 4 Tension-tension fatigue behavior of CARALL laminate

The S-N data for CARALL is shown in Fig. 4, as a plot of the maximum fatigue stress against the number of cycles to failure. The plots of these metal/fiber composites are almost linear over the range of fatigue life up to 10^6 cycles. It can be observed in this figure that for both aluminum surface treatments, the fatigue results when evaluated in high cycle, were similar. This result confirms the microscopic observation and tensile results can be observed that both treatments presented similar characteristics and, can be used as an effective treatment over the aluminum surface to promote the structural adhesion. During this work, it was observed that CF/E laminate presented higher fatigue resistance values in low cycles, but presents a similar behavior in high cycles, when compared with MFLs.

Figure 5 shows the comparison of the fatigue performance based on the relationship between the normalized fatigue stress and the fatigue cycles. The fatigue performance of the CARALL processed with CAA treatment is

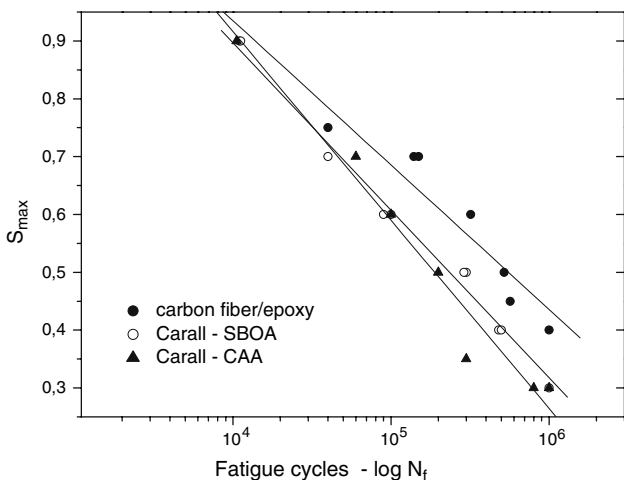


Fig. 5 Fatigue performance for normalized maximum fatigue stress in function of fatigue cycles

comparable to the fatigue performance of CARALL obtained with SBOA treatment. As the fatigue performance based on the normalized and absolute applied stress gives similar results and conclusions, it is important for structural or material engineers to consider both approaches. According to Fig. 5 can be observed that CF/E laminates present a different normalized fatigue curve due probably to the contribution of aluminum alloy on MFLs.

It is well established that the fiber-reinforced plastics are significantly different from their metal counterparts in terms of their structural makeup and in the manner by which fatigue fracture initiates and develops during cyclic loading. Figures 6 and 7 depicted the photomicrography of

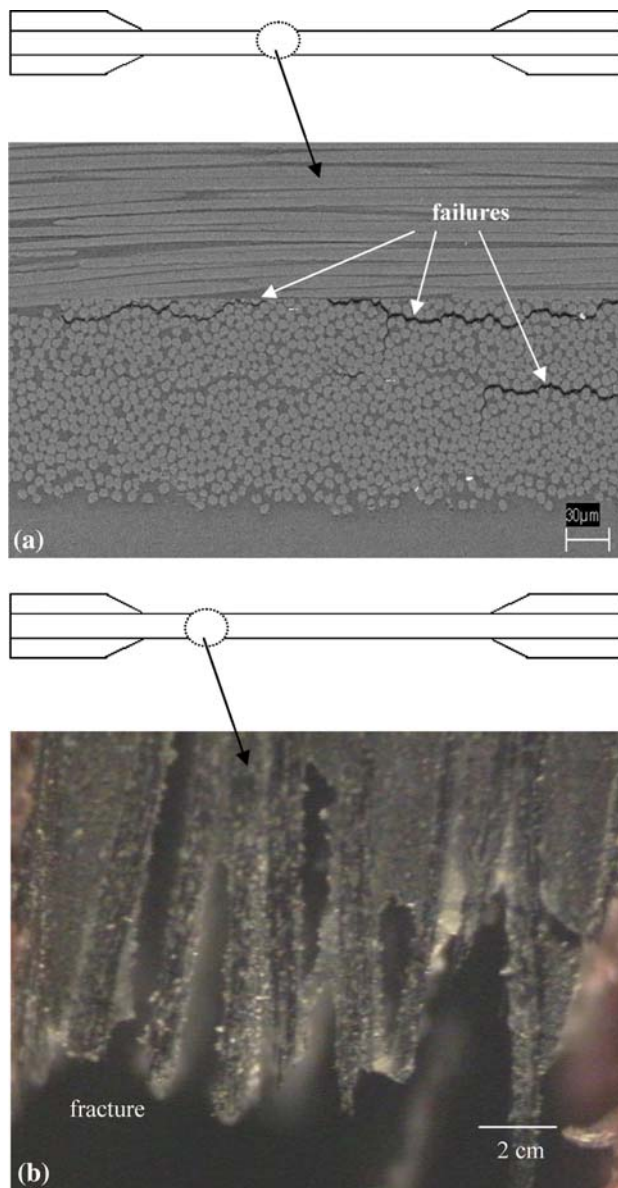


Fig. 6 SEM fractography shows carbon fiber/epoxy composite fracture: (a) under 380 MPa (*lateral view*) and (b) under 200 MPa (*transversal view*)

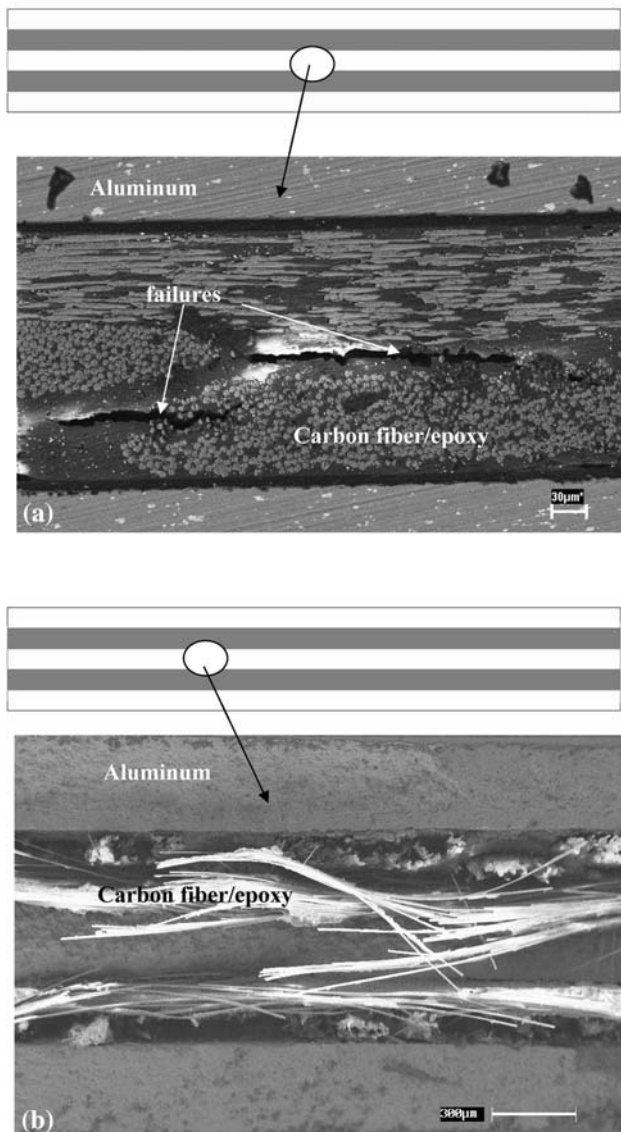


Fig. 7 SEM fractography shows CARALL fracture: (a) under 380 MPa (*lateral view*) and (b) under 200 MPa (*transversal view*)

CF/E and CARALL, respectively, after fatigue load. In this Fig. 6 can be evidenced the complex modes in which the fatigue failure occurs in plain weave woven carbon fabric reinforced epoxy matrix composite used as component in the metal/fiber composite for the present study. Both Figs. 6 and 7 shows the matrix and fibers cracks in $0/90^\circ$. Figures 6a and 7a show the specimens under high cycle. This damage can be considered as initiation of the fatigue damage process, which is followed by a sequence of the microdamage events that ultimately lead to the final fatigue failure. This subsequent damage sequence is responsible for a continuous reduction in modulus and strength during fatigue loading. Under low cycle (high stress), can be observed a catastrophic damage (Figs. 6b and 7b). For both

cases, low and high cycles, it was observed a catastrophic damage for CARALL specimens after to be submitted to fatigue load.

Conclusion

The fatigue behavior of CF/E laminate and CARALL were investigated by fatigue tests under constant amplitude loading. Two kinds of treatments were done over aluminum alloy (CAA and SBOA) to process CARALL specimens.

Results obtained by SEM evaluation, tensile and fatigue tests showed that both treatments presented similar results and can be used as surface treatments to guarantee a good structural adhesion between the aluminum 2024-T3 alloy and continuous fiber/epoxy composites.

According to the microscopy evaluation, crack in $0/90^\circ$ was found to be the major damage mode in plain weave carbon fabric reinforced plastic laminates. On the other hand, it was observed by SEM that in specimens of CARALL analyzed in high cycle (low stress), the initial fracture occurred on the aluminum alloy, without the CF/E failure.

Acknowledgement The authors acknowledge financial support received from FAPESP under grant 05/54358-7.

References

1. Vlot A, Gunnink JW (2001) Fibre metal laminates. Kluwer Academic Publishers, Delft, the Netherlands
2. Soprano A, Apicella A, D'Antonio L, Schettino F (1996) Int J Fatigue 18(4):265
3. Botelho EC, Campos AN, Barros E, Pardini LC, Rezende MC (2005) Composites B 37(2–3):255
4. Jang BZ (1994) Advanced polymer composites: principles and applications. 1st edn, ASM International, OH, USA
5. Lin CT, Kao PW (1996) Composites A 27A:9
6. Silva RA, Botelho EC, Pardini LC, Rezende MC (2004) J Appl Adhesion Technol 18:1799
7. Botelho EC, Pardini LC, Rezende MC (2005) Mater Sci Eng A 399:190
8. Taranets NY, Jones H (2004) J Mater Sci 39(18):5727
9. De Rosa RL, Grant JT, Katsen L et al (2000) Corrosion 56(4):395
10. Silva RA, Botelho EC, Rezende MC, Pardini LC (2006) Mater Res 9:247
11. Carrino L, Napolitano G, Sorrentino L (2006) Intl J Adv Manuf 34:465
12. Polini W, Sorrentino L (2003) Appl Surface Sci 214:232
13. Kawai M, Hachinohe A, Takumida K, Kawase Y (2001) Composites A 32:13–23
14. Khan Z, Al-Sulaiman, Farooqi JK (1998) J Reinforced Plastics Comp 17:1320
15. Wyzgoski MG, Novak GE (1995) Polym Comp 16:38
16. Ryan L, Monaghan J (2000) J Mater Process Technol 103:36
17. Reyes G, Cantwell WJ (2000) Compos Sci Technol 60:1085

18. Davies P, Ducept F, Brunner AJ, Blackman BRK, Morais AB (1996) In: Seventh European conference on composite materials, London, UK, pp 14–16
19. Zweben C, Hahn HT, Chou T-W (1989) Mechanical behavior and properties of composite materials, delaware composites design encyclopedia, vol. 1. Lancaster, Pennsylvania, USA
20. Atodaria DR, Putatunda SK (1997) *J Comp Mater* 31(18):18
21. Dagallaix G, Hassaïni D, Vittecoq E (2002) *Intl J Fatigue* 24:319
22. Gregory JR, Spearing SM (2005) *Composites A* 36:665
23. Botelho EC, Lauke B, Figiel L, Rezende MC (2003) *Comp Sci Technol* 63:1843
24. Bureau MN, Denault J (2004) *Comp Sci Technol* 64:1783
25. Lin CT, Kao PW (1996) *Acta Mater* 44(3):1181
26. Davis JR (1993) *Aluminum and aluminum alloys*. ASM International, Metals Park, OH, USA